ELSEVIER

Journal of Photochemistry and Photobiology A: Chemistry 145 (2001) 93–99

Journal of Photochemistry and Photobiology A:Chemistry

www.elsevier.com/locate/jphotochem

Surface characterization and photochemical behavior of poly(ethylene terephthalate) and TiO_2/poly(ethylene terephthalate) interface by using sum-frequency generation

Takayuki Miyamae, Hisakazu Nozoye*

Nanotechnology Research Institute, National Institute of Advanced Industrial Science and Technology (AIST), 1-1 Higashi, Tsukuba, Ibaraki 305-8565, Japan

Received 14 March 2001; received in revised form 14 May 2001; accepted 1 June 2001

Abstract

The surface molecular orientation, buried interface characterization of biaxially stretched poly(ethylene terephthalate) (PET) film, and its photochemical behavior by UV irradiation have been investigated by using infrared–visible sum-frequency generation (SFG). The SFG spectra of PET surface showed a pronounced peak at 1705 cm^{-1} which is characteristic of the C=O stretching vibration in an ester function. The SFG spectra indicate that the polymer chains at the surface appear to be well aligned parallel to the surface plane. By depositing a TiO_2 film, the C=O and the C=C bonds of PET are tilted from the surface plane. Change of the molecular orientational conformation distribution is also observed in the case of TiO_2/PET interface. In contrast to the case of TiO_2/PET, deposition of SiO_2 film on PET surface does not induce changes in the molecular orientational conformation. By irradiating UV pulses, photo-degradation of PET is observed for TiO_2/PET interface, while such degradation is not observed in PET surface and SiO_2/PET interface.

Keywords: Surface characterization; Photochemical behavior; Poly(ethylene terephthalate); TiO_2/PET interface; Sum-frequency generation

1. Introduction

Polymeric films coated with inorganic thin films have many useful properties such as antireflective and protective optical coatings, gas barrier coatings for food and pharmaceutical packaging industry, and numerous applications in visor, automobile industry, and so on. For the application to the liquid crystalline display as protective optical coatings, it is important to the interface interaction between polymer and inorganic coatings and its photo-protective properties. Physicochemical interaction between metals and polymers has been widely studied with X-ray photoemission spectroscopy (XPS) [1–4], near-edge X-ray absorption spectroscopy (NEXAFS) [5], and high-resolution electron energy loss spectroscopy (HREELS) [6]. Oxide/polymer interfaces and the mechanism of the photo-induced reaction have been also extensively studied for many years by using many different techniques such as IR, Raman spectroscopy, XPS [7,8], and atomic force microscopy (AFM). Some of these techniques require UHV environment, others are not surface-sensitive or cannot provide interface information at the molecular level.

Recently, sum-frequency generation (SFG) vibrational spectroscopy has been demonstrated to be an effective surface and interface analytical probe [9–11]. Since SFG is second-order nonlinear optical process, the process is electric-dipole forbidden in a bulk with inversion symmetry, but allowed at interface where the inversion symmetry is broken. Therefore, it is particularly sensitive to the interfacial structure between two centrosymmetric media. The resonant enhancement of the SF signal occurs when the input IR frequency agrees with a vibrational mode that is both IR- and Raman-active. Furthermore, input/output polarization dependence of the spectra provides information about average orientation of interface molecules. Thus, this spectroscopic technique is ideal for studies of chemical composition and structure of polymer surface [12–16]. In other words, SFG provides detailed information of the polymer surface at the molecular level and can be used to study any polymer surface or interface that can be accessed by light.

In this work, we report the molecular conformations of the biaxially stretched PET surface and the buried interface of TiO_2/PET by using SFG. In general, polymers have the advantage of having high mechanical strength combined with

* Corresponding author. Tel.: +81-298-614527; fax: +81-298-614504.
E-mail address: h.nozoye@aist.go.jp (H. Nozoye).

1010-6030/01/$ – see front matter
PII: S1010-6030(01)00559-7

a low density and good transparency in the visible region. However, they present a rather high softness and are easily damaged. Deposition of TiO_2 thin films would certainly improve these low mechanical and optical properties. Especially, TiO_2 presents very remarkable characteristics not only thanks to its chemical stability but also to its excellent properties. It has a high refractive index ($n = 2.5$) and good optical transmittance in the visible (below 380 nm) and in the infrared region. Therefore, good photo-protective properties are expected by the deposition of TiO_2 films on PET because UV irradiation leads to changes in the surface of PET as a result of photo-oxidation [17], photo-degradation [18], and photo graft reaction [19]. Furthermore, TiO_{2-x} compounds have semiconducting properties depending on the oxygen vacancy concentration [20]. Thus TiO_2, particularly as thin films, shows much potential for various applications, such as photocatalytic devices [20,21], electrochromic properties [22], gas sensors [23], interference filters and antireflection coatings [24], and dielectrics in optoelectronic [25] and electronic devices.

By using the SFG technique, we investigate the changes of the molecular structure at TiO_2/PET interface. For the sake of comparison, we also measured the SFG spectra of SiO_2/PET interface. The difference between SiO_2- and TiO_2-deposited PET interface is discussed. We also investigate the effect of UV irradiation to the TiO_2/PET interface. In particular, from the irradiation of UV pulses to the TiO_2/PET system, we could successfully observe the photo-induced interface reaction. Our aim is to elucidate potential applicability of SFG to the characterization of the buried interface of oxide/polymer system.

2. Experimental

Samples of biaxially stretched PET films without additives used in this study were supplied from Film Research Laboratories of Teijin Limited. Their thicknesses were 100 μm. Unoriented film was drawn in one direction, defined as the machine direction (MD), to a draw ratio of 4. Subsequently, it was drawn in the transverse direction (TD) to a draw ratio of 4 or larger. Samples were taken from both the center part and the edge part of the film. It is well known that the sequentially, biaxially drawn films have optical anisotropy, and the molecular orientation is different at each point across the TD [26,27].

Titanium dioxide films deposited on PET substrates were prepared by oxygen-radical beam-assisted deposition [28,29]. Titanium was evaporated from an electron beam source. Titanium and oxygen radical beam were simultaneously impinged on PET films at room temperature. Typical Ti evaporation rate was 0.1 nm/s. The thickness of TiO_2 was about 30 nm, as monitored by a quartz thickness monitor. Details of an oxygen-radical beam source were described elsewhere [28]. The flux of oxygen-radical beam from the oxygen-radical beam source was 3.8×10^{15} radicals $cm^{-2}\ s^{-1}$, which was determined by monitoring the change of the resonant frequency of a Ag-precoated quartz crystal [30]. We also deposited a silicone dioxide film onto a PET film. In this case, silicon dioxide (fused silica) was used as a target of the electron beam source. Typical SiO_2 evaporation rate was 0.1 nm/s. The thickness of SiO_2 was about 30 nm.

In IR–visible SFG experiments, a mode-locked Nd:YAG laser (EKSPLA PL2143D) with 30 ps pulse width and 10 Hz repetition rate was used as a master light source. A tunable IR beam was generated by a $AgGaS_2$ crystal by difference frequency mixing of the fundamental of Nd:YAG laser with the output of an optical parametric generator (OPG; EKSPLA PG401VIR/DFG) pumped by the third harmonics of the YAG laser. The frequency of the IR beam was calibrated using a standard polystyrene film. The visible (532 nm) and

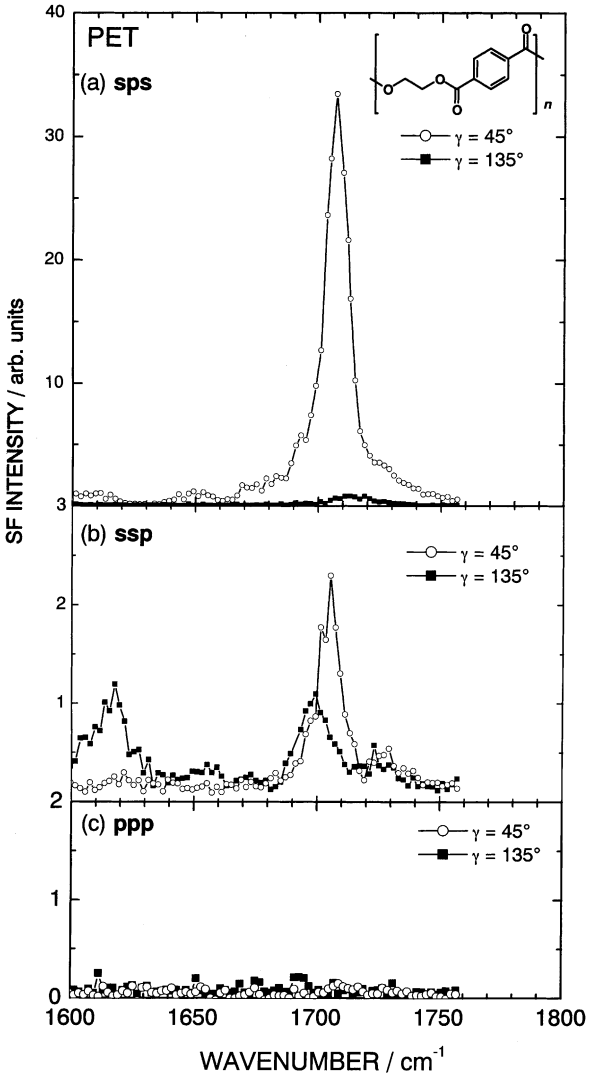

Fig. 1. SFG spectra of PET surface in the C=O stretching range in three different polarization combinations for (a) sps (for s-, p- and s-polarized SF output, visible input, and IR input, respectively), (b) ssp, and (c) ppp, at $\gamma = 45°$ and 135°.

IR beams were overlapped at the sample surface spatially and temporally with the incidence angles of 70° and 50°, respectively. Pulse energies and beam sizes were about 1 mJ and 0.4 mm for the visible input and 50–200 μJ and 0.5 mm for the infrared input, respectively. Spectral bandwidth of the IR pulses was $\sim$10 cm^{-1}. The SFG spectra were normalized for infrared and visible intensity variations, respectively.

3. Results and discussion

We have measured SFG surface vibrational spectra of PET in the C=O stretching region. The SFG spectra of the PET film taken from the edge part were measured in different input/output polarization combinations at different sample orientations specified by the azimuthal angle γ between the common incidence plane of the visible and IR beams and the MD direction. The spectra at $\gamma = 45°$ and 135° are presented in Fig. 1. The SFG spectra in sps polarization combination (i.e., s-polarized SFG output, p-polarized visible input, and s-polarized IR input, respectively) exhibit a pronounced peak at 1705 cm^{-1}. The main peak at 1705 cm^{-1} is originated from the C=O stretching vibration in an ester moiety. In ssp polarization combination, two peaks are observed at 1705 and 1725 cm^{-1} at $\gamma = 45°$, and another two peaks are observed at 1615 and 1693 cm^{-1} at $\gamma = 135°$. The peak at 1693 cm^{-1} is assigned to the C=O stretching vibration of benzoic acid, characteristic of the terminal acidic function of the polymer [31]. In ppp polarization combination, SFG signal is hardly distinguishable from noise, as shown in Fig. 1(c). In Fig. 2, we show the polar plot of square root of SFG intensity of C=O stretching mode (1705 cm^{-1}) for the edge and the center part of the film as a function of γ in sps polarization combination. In the edge part of the film, the intensity of the C=O stretching mode is maximum at around $\gamma = 45°$.

The band at 1615 cm^{-1} is derived from the C=C stretching vibration of phenyl ring (A_g symmetry) [32]. The phenyl ring of PET ($-CO-C_6H_4-CO-$) has D_{2h} symmetry, which has inversion symmetry, and the A_g mode is IR-inactive and, therefore, SFG-inactive. In the case of the *cis*-isomer of terephthalate moiety, which is contained in the amorphous region, the symmetry reduces to the C_{2v} configuration. In this case, the C=C stretching mode of phenyl ring is active in

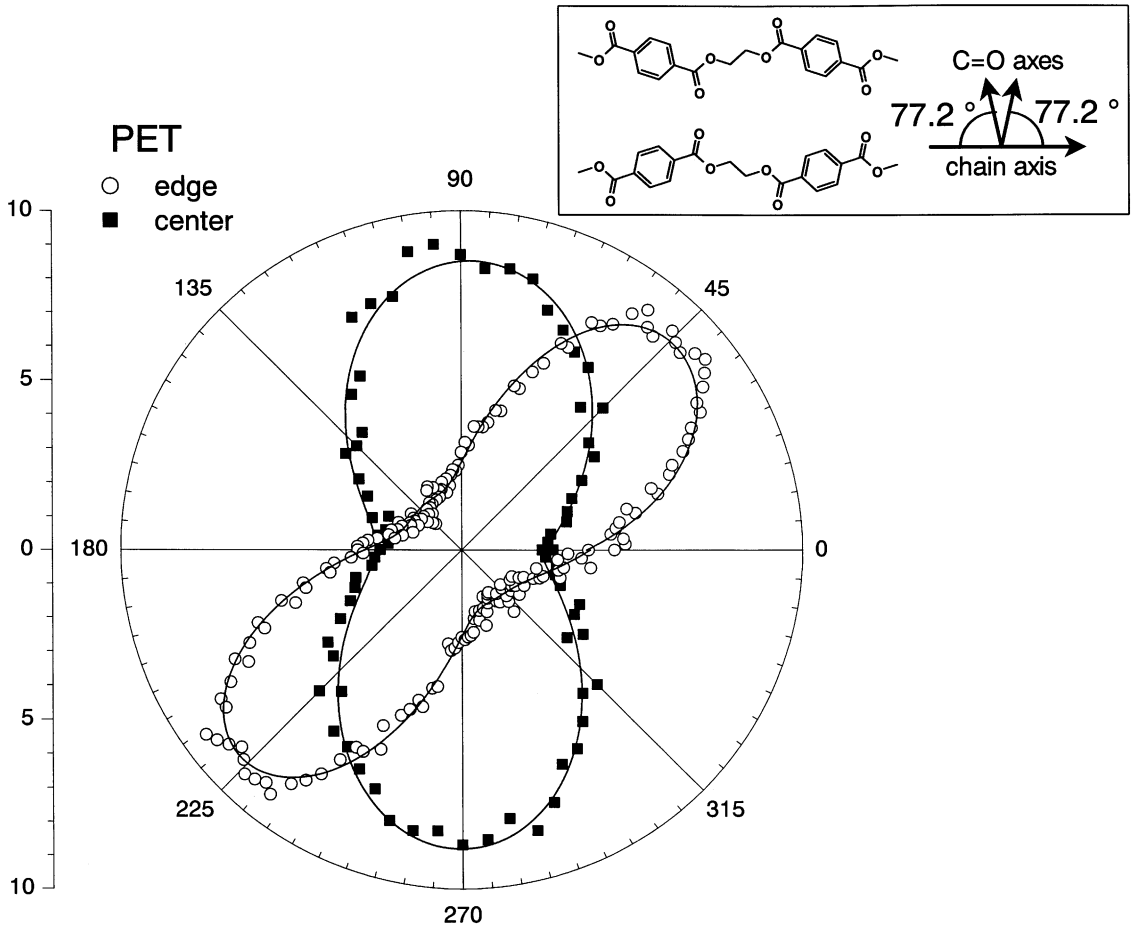

Fig. 2. Square root of the SF intensity of the C=O stretching mode vs. sample rotation angle ϕ for the edge and the center part of the PET film. $\phi = 0°$ defines the MD direction of the film. Solid lines correspond to calculated fits to the data.

both Raman and IR by the reduction of the symmetry from D_{2h} to C_{2v}. The biaxially stretched film is known to have bulk crystallinity of ~56% [33]. Thus, we conclude that the peak at 1615 cm^{-1} is originated from the phenyl C=C stretching vibration of the amorphous part of the surface region.

From the SFG spectra, we can obtain definitive information of the surface molecular orientation of PET. Generation of the SF signal for the C=O stretching mode requires an IR polarization component parallel to the C=O axis. The fact that the mode is very strong in sps spectra (at $\gamma = 45°$) and absent in ppp spectra indicates that the C=O axis must be parallel to the surface plane. This result is in good agreement with the result of NEXAFS of biaxially stretched PET [34,35]. Since the C=O stretching mode is very strong at $\gamma = 45°$, and almost absent at $\gamma = 135°$, we conclude that the PET chains are well aligned along $\gamma = 45°$ in the edge part of the film. In fact, it is well known that the sequentially, biaxially drawn PET film shows optical anisotropy, and the molecules tend to align along some direction in the edge region of the films [26,27]. In the case of the PET sample taken from the center part, the intensity of the C=O stretching mode is maximum at around $\gamma = 90°$, as shown in Fig. 2. This result indicates that the PET chains are almost parallel to the TD direction. These molecular orientation distributions along TD direction are in good agreement with the results of the birefringence measurements of biaxially stretched PET films [26]. It should be noticed that the two possible molecular orientational conformations should exist at the surface region, as depicted in the inset of Fig. 2. From the data of Daubeny et al. [36], the angle between C=O axis and the chain axis is determined to be 77.2°. The distribution of the molecular orientation angle ϕ can be deduced when we assume a Gaussian distribution for ϕ:

$$f(\phi) = \sum_i C_i \exp\left[-\frac{(\phi - \phi_{0_i})^2}{2\sigma_{\phi_i}^2}\right], \quad (1)$$

where C_i is a normalization constant, ϕ_{0_i} the average value of ϕ, and σ_{ϕ_i} the variance. Better fitting curves are obtained by considering two C=O axes. The solid lines in Fig. 2 illustrate the fitted curves by Eq. (1) assuming the presence of the two C=O axes, which are inclined to the maximum intensity of the angle ϕ, respectively. The calculated, averaged orientational distribution of the chain axes are $\sigma_\phi = 17.9 \pm 0.6°$ and $\sigma_\phi = 32.1 \pm 0.9°$ for the edge and center part of the films, respectively. A significantly higher degree of order is observed for the sample from the edge part of the film. The variation of the orientation distribution may cause the non-uniformity of physical properties across the TD of the film.

In Fig. 3, we show the SFG spectra of the TiO_2/PET interface prepared by oxygen-radical beam-assisted TiO_2 film deposition on a PET substrate, which was taken from the edge part. The peak intensities of the C=O and C=C stretching modes do not change after the deposition of TiO_2

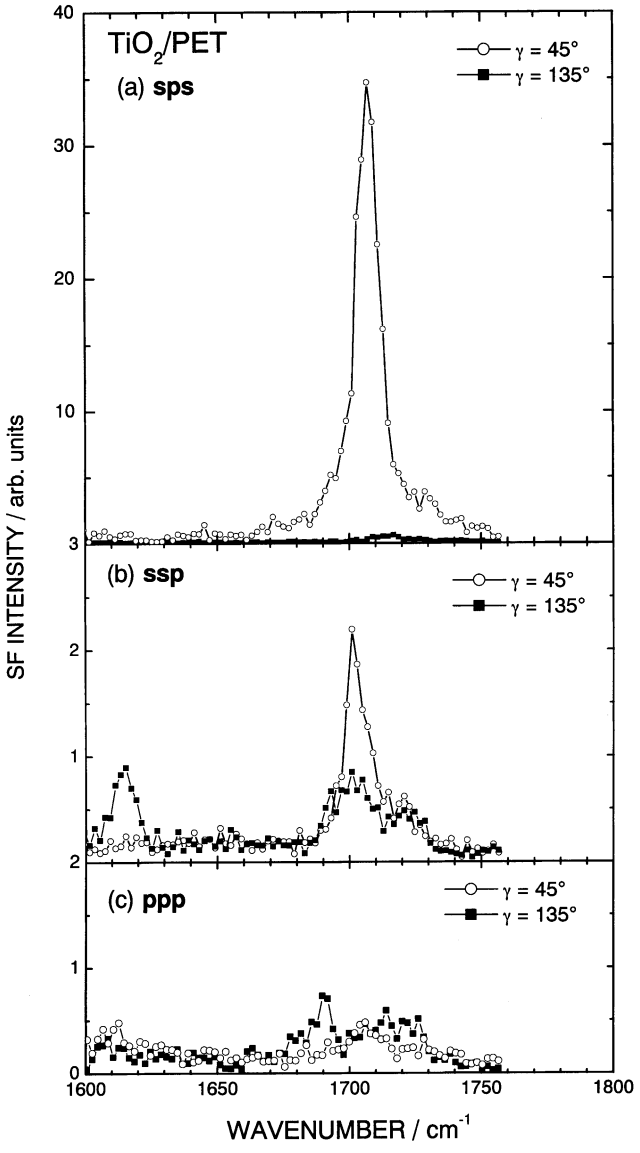

Fig. 3. SFG spectra of PET after deposition of TiO_2 by oxygen-radical beam-assisted method in three different polarization combinations for (a) sps, (b) ssp, and (c) ppp, at $\gamma = 45°$ and 135°.

film, as shown in Figs. 3(a) and (b). In the case of the SFG spectra of the PET surface exposed to the oxygen-radical beam, however, the intensities of the C=O and C=C stretching mode are reduced [37]. The oxygen-radical exposure induces the ring-opening reaction leading to new oxygen-containing species formation accompanied by consecutive loss of aromatic character of the polymer surface. Such effect is small in the case of TiO_2-deposited PET, since PET surface is protected by TiO_2 deposited on it. In ppp polarization combination, both C=C and C=O stretching modes are appeared, as shown in Fig. 3(c). The appearance of these bands in ppp polarization combination indicates that the C=O and the C=C axes are tilted from the surface plane. This result clearly shows that the TiO_2 film deposited by the oxygen-radical beam-assisted method changes the

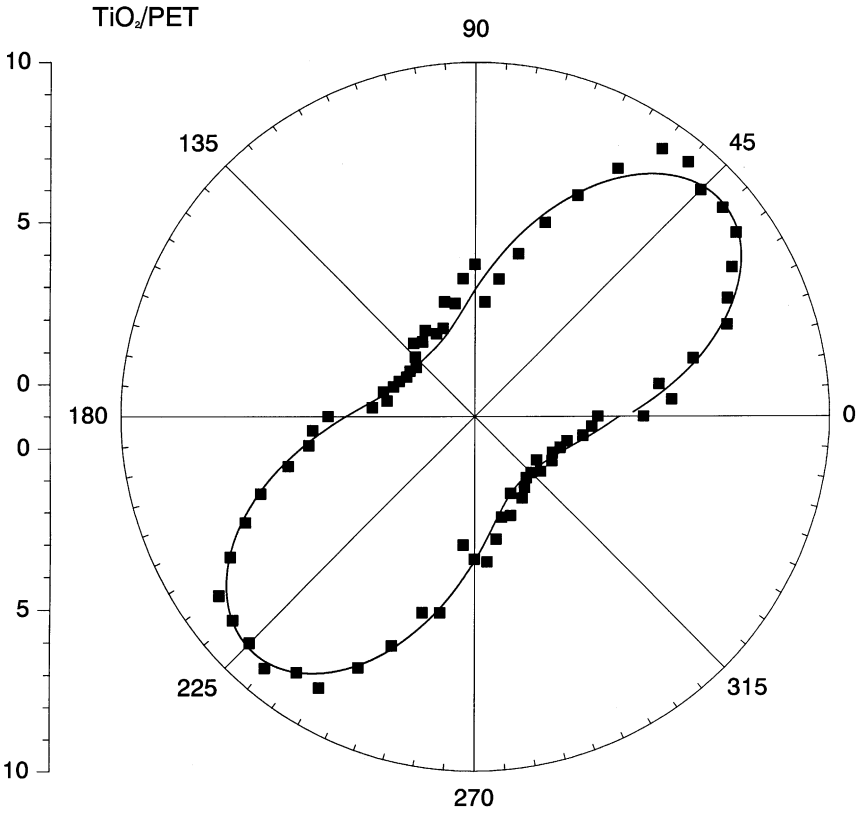

Fig. 4. Square root of the SF intensity of the C=O stretching mode vs. sample rotation angle ϕ for the PET film after deposition of TiO_2 by oxygen-radical beam-assisted method. $\phi = 0^\circ$ defines the MD direction of the film. Solid line corresponds to a calculated fit to the data.

conformation of the molecular chains of PET. In Fig. 4, we show the polar plot of square root of SFG intensity of C=O stretching mode observed from the TiO_2/PET interface as a function of γ in sps polarization combination. The calculated, averaged orientational distribution of the chain axis is $\sigma_\phi = 23.2 \pm 1.4^\circ$, which is larger than that in the case of neat PET. Change of the molecular distribution indicates that the deposition of TiO_2 film induces structural modification to the PET surface. It should be noticed that such structural modification is not observed in the case of the PET surface after the oxygen-radical beam exposure.

Fig. 5 shows the SFG spectra of the SiO_2/PET interface. In contrast to the case of the TiO_2/PET interface, there are no bands in ppp polarization combination, indicating that deposition of SiO_2 film on the PET surface does not induce changes in the molecular conformation of PET. Thus, we conclude that the TiO_2/PET and SiO_2/PET interfaces take different molecular conformation. The calculated, averaged orientational distribution of the chain axis obtained from the polar plot of square root of SFG intensity of C=O stretching mode is $\sigma_\phi = 21.5 \pm 1.2^\circ$.

Finally, we show the effects of UV laser radiation on the PET surface and the TiO_2/PET interface. In Figs. 6(a) and (b), we show the change of the SFG spectra of the C=O region of PET after irradiation of the third harmonics (λ = 355 nm) of Nd:YAG laser with 30 ps duration. The radiation energy was set to 9 mJ/cm^2. Its wavelength corresponds to energy of 3.49 eV, which is slightly higher than the valence to conduction band energy gap of 3.08 eV for rutile [38]. On radiation of 355 nm, the C=O mode does not change for the PET surface, as shown in Fig. 6. After irradiation of 2000 shots, however, a partial swelling occurred. The intensity of C=O mode is decreased after UV irradiation to TiO_2/PET, as shown in Figs. 6(c) and (d). This result indicates that TiO_2 film accelerates the photo-degradation reaction of PET. The photo-degradation of PET by UV irradiation of wavelength 312 nm proceeds mainly by the mechanism of photo-Fries rearrangement to form three-dimensional networks by the primary photolysis process and subsequent photo-oxidation reaction, resulting in the cleavage of main chains [39]. The wavelength of 355 nm has no sufficient energy to cause the initiation of the photo-degradation, since PET has no absorption at 355 nm. For the sake of comparison, we also measured the SFG spectra of SiO_2/PET after UV irradiation. On radiation of 355 nm, the C=O mode does not change for the SiO_2/PET system, because PET has no absorption at 355 nm and the bandgap of SiO_2 is 8.95 eV [40]. Therefore, this reaction should not be originated from the photo-induced reaction of PET itself. Details of the mechanism of the photo-degradation process of TiO_2/PET interface is not clear; however, the photo-generated valence band holes in TiO_2 deposited on PET may induce the degradation of

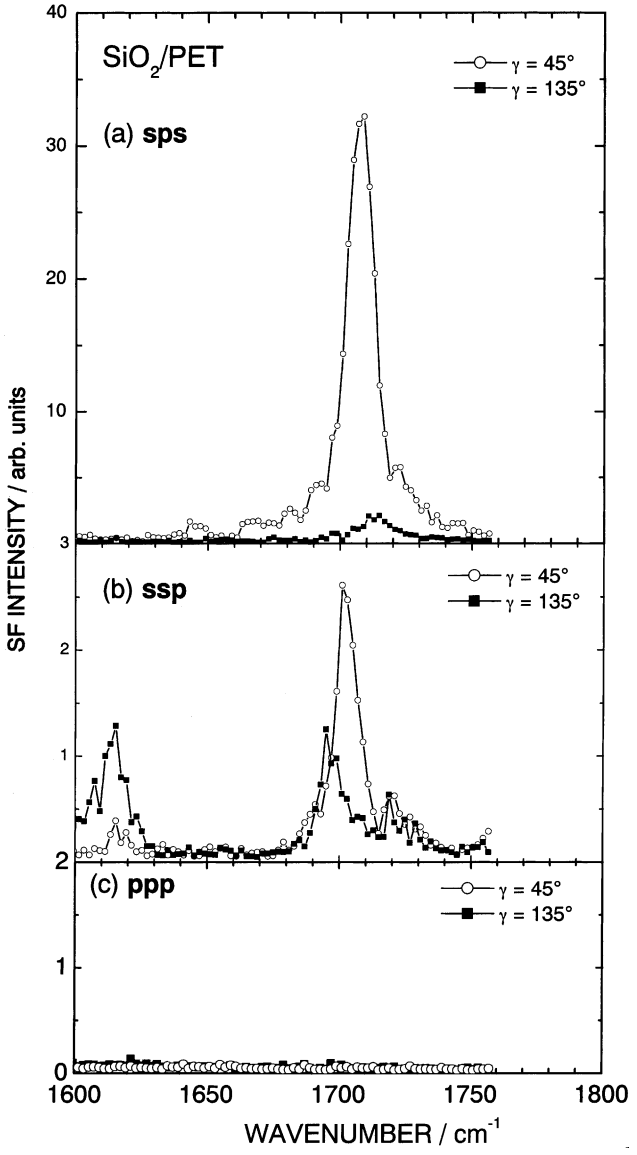

Fig. 5. SFG spectra of PET after deposition of SiO_2 film in three different polarization combinations for (a) sps, (b) ssp, and (c) ppp, at $\gamma = 45°$ and 135°.

polymer chain at the TiO_2/PET interface and the nucleation of the radicals, which form the three-dimensional networks.

In conclusion, the surface molecular conformations of the biaxially stretched PET films and characterization of the buried interface of TiO_2/PET have been investigated by using SFG. The SFG spectra show that the polymer chains at the surface appear to be well aligned parallel to the surface plane with C=O parallel to the surface plane. By depositing the TiO_2 film, the C=O and the C=C bonds of PET are tilted from the surface plane. In contrast to the case of TiO_2/PET, deposition of SiO_2 film on PET surface does not induce changes in the molecular conformation of PET. By irradiating UV pulses (355 nm), we could successively observe the photo-degradation of the C=O moiety of PET for TiO_2/PET interface, while such photo-induced

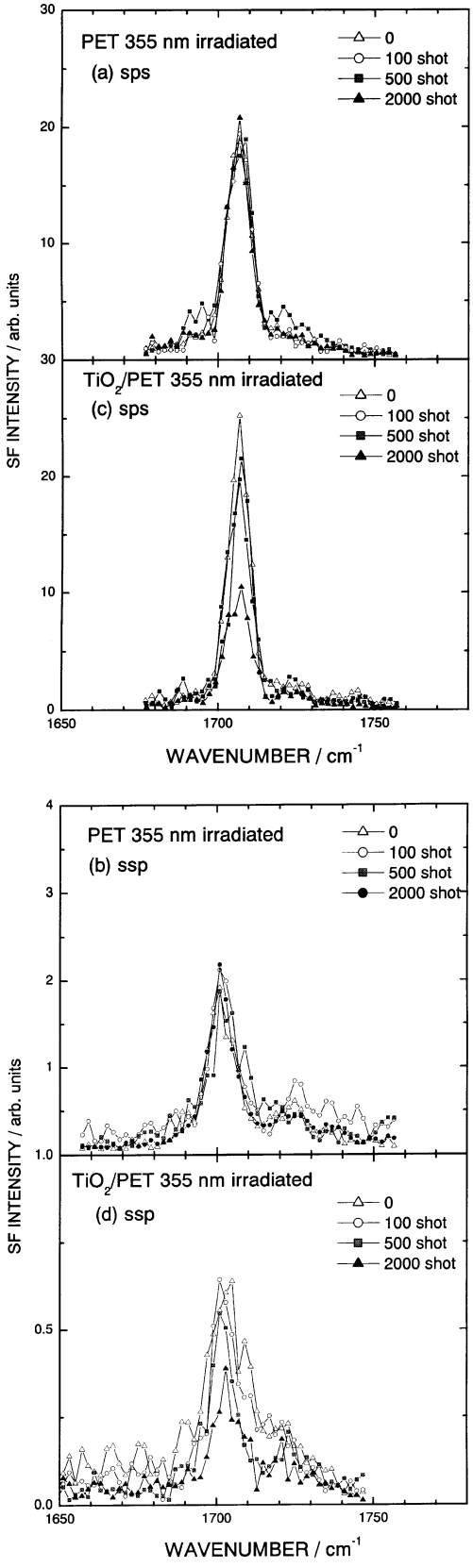

Fig. 6. Change of the SFG spectra of UV (355 nm)-irradiated PET and TiO_2/PET in (a) sps and (b) ssp combinations for PET, and in (c) sps and (d) ssp combinations for TiO_2/PET, respectively. Spectra at $\gamma = 45°$ are shown.

degradation is not observed in PET surface and SiO_2/PET interface.

Acknowledgements

The authors would like to thank Drs. Masao Hirasaka and Kazuhiko Sato of Teijin Limited for supplying the PET films.

References

[1] B.M. Dekoven, P. Hagans, Appl. Surf. Sci. 27 (1986) 199.
[2] J.L. Jordan, C.A. Kovac, J.F. Morar, R.A. Pollak, Phys. Rev. B 36 (1987) 1369.
[3] N.J. Chou, C.H. Tang, J. Vac. Sci. Technol. A 2 (1984) 751.
[4] J.F. Silvain, A. Arzur, M. Almot, J.J. Ehrhardt, P. Lutgen, Surf. Sci. 251/252 (1991) 787.
[5] J.F. Friedrich, I. Koprinarov, R. Giebler, A. Lippitz, W.E.S. Unger, J. Adhesion 71 (1999) 297.
[6] J.J. Pireaux, P.A. Thiry, R. Caudano, P. Pfluger, J. Chem. Phys. 84 (1986) 6452.
[7] J.C. Rotger, J.J. Pireaux, R. Caudano, N.A. Thorne, H.M. Dunlop, M. Benmalek, J. Vac. Sci. Technol. A 13 (1995) 260.
[8] S.B. Amor, G. Baud, M. Benmalek, H. Dunlop, R. Frier, M. Jacquet, J. Adhesion 65 (1998) 307.
[9] Y.R. Shen, In the Principle of Nonlinear Optics, Wiley, New York, 1984.
[10] Y.R. Shen, Annu. Rev. Phys. Chem. 40 (1989) 327.
[11] K. Domen, C. Hirose, Appl. Catal. 160 (1997) 153.
[12] D. Zhang, Y.R. Shen, G.A. Somorjai, Chem. Phys. Lett. 281 (1997) 394.
[13] D. Zhang, R.S. Ward, Y.R. Shen, G.A. Somorjai, Phys. Chem. B 101 (1997) 9060.
[14] D.H. Gracias, D. Zhang, L. Lianos, W. Ibach, Y.R. Shen, G.A. Somorjai, Chem. Phys. 245 (1999) 277.
[15] X. Wei, X. Zhuang, S. Hong, T. Goto, Y.R. Shen, Phys. Rev. Lett. 82 (1999) 4256.
[16] D. Kim, Y.R. Shen, Appl. Phys. Lett. 74 (1999) 3314.
[17] D.K. Owens, J. Appl. Polym. Sci. 19 (1975) 3315.
[18] P. Blais, M. Day, D.M. Wiles, J. Appl. Polym. Sci. 17 (1973) 1985.
[19] S. Takezoe, T. Matoba, H. Kimura, ACS Symp. Ser. 121 (1980) 217.
[20] A. Ohmori, K.C. Park, M. Inuzuka, Y. Arata, K. Inoue, N. Iwamoto, Thin Solid Films 201 (1991) 1.
[21] M.C. Asensio, M. Kerkar, D.P. Woodruff, A.V. de Carvalho, A. Fernandez, A.R. Gonzalez-Elipe, M. Fernandez-Garcia, J.C. Conesa, Surf. Sci. 273 (1992) 31.
[22] N. Özer, Thin Solid Films 214 (1992) 17.
[23] A. Brunik, H. Czternastek, K. Zakrzewska, M. Jachimowski, Thin Solid Films 199 (1991) 279.
[24] K. Bange, C.R. Ottermann, O. Anderson, U. Jeschkowski, M. Laube, R. Feile, Thin Solid Films 197 (1991) 279.
[25] V.P. Gupta, N.M. Ravindra, J. Phys. Chem. Solids 41 (1980) 591.
[26] K. Sakamoto, Kobunshi Ronbunshu 48 (1991) 671.
[27] G.H. Kim, C.-K. Kang, C.G. Chang, D.W. Ihm, Eur. Polym. J. 33 (1997) 1633.
[28] F. Imai, K. Kunimori, H. Nozoye, J. Vac. Sci. Technol. A 13 (1995) 2508.
[29] Y. Yamada, T. Harada, H. Uyama, T. Murata, H. Nozoye, Thin Solid Films 377–378 (2000) 92.
[30] V. Matijasevic, E.L. Garwin, R.H. Hammond, Rev. Sci. Instrum. 61 (1990) 1747.
[31] P. de Donato, J.M. Cases, B. Humbert, P. Lutgen, F. Feyder, J. Polym. Sci. B 30 (1990) 1305.
[32] M.C. Tobin, J. Phys. Chem. 61 (1957) 1392.
[33] G. Beamson, D.T. Clark, N.W. Hayes, D.S.-L. Law, V. Siracusa, A. Recca, Polymer 37 (1996) 379.
[34] I. Ouchi, I. Nakai, M. Kamada, S. Tanaka, J. Electron. Spectrosc. Relat. Phenom. 78 (1996) 363.
[35] I. Koprinarov, A. Lippitz, J.F. Friedrich, W.E.S. Unger, Ch. Wöll, Polymer 38 (1997) 2005.
[36] R.P. Daubeny, C.W. Bunn, C. Brown, J. Proc. R. Soc. A 226 (1954) 531.
[37] T. Miyamae, Y. Yamada, H. Uyama, H. Nozoye, Surf. Sci., in press.
[38] F.A. Grant, Rev. Mod. Phys. 31 (1959) 646.
[39] E. Fujimoto, T. Fujimaki, Kobunshi Ronbunshu 52 (1995) 378.
[40] S. Miyazaki, H. Nishimura, M. Fukuda, L. Ley, J. Ristein, Appl. Surf. Sci. 113/114 (1997) 585.